# Vortex properties in superconducting Nb/Pd multilayers

C. Coccorese, C. Attanasio, L. V. Mercaldo, M. Salvato, and L. Maritato
*Dipartimento di Fisica and INFM, Università degli Studi di Salerno, Baronissi (Sa), I-84081, Italy*

J. M. Slaughter and C. M. Falco
*Department of Physics and the Optical Sciences Center, University of Arizona, Tucson, Arizona 85721*

S. L. Prischepa
*State University of Informatics and RadioElectronics, P. Brovka str. 6, Minsk, 220027, Belarus*

B. I. Ivlev
*Universidad Autonoma de San Luis Potosi, Instituto de Fisica, A. Obregon 64, 78000 San Luis Potosi, S.L.P., Mexico*
(Received 14 May 1997; revised manuscript received 31 October 1997)

We have investigated the upper critical magnetic field $H_{c2}$, the critical current density $J_c$, and the pinning force $F_p$ in sputtered Nb/Pd multilayers, varying the temperatures $T$, the Pd thicknesses $d_{\mathrm{Pd}}$ and the magnetic field $H$ orientation (parallel and perpendicular to the plane of the sample). In perpendicular fields, the vortex dynamics was strongly influenced by grain-boundary pinning. In parallel fields, a peak was observed in the $J_c(H)$ curves for samples with Pd thicknesses $d_{\mathrm{Pd}} > 100$ Å. After comparing the experimental results with the existing theories, we have related the presence of this peak effect to the matching of vortex kinks with the layered artificial structure. [S0163-1829(98)05210-2]

## I. INTRODUCTION

In recent years artificially layered superconducting systems have been extensively studied to investigate the influence of the reduced dimensionality on different physical properties (critical temperature, penetration depth, pinning forces) and to obtain, viewed as test systems, much information on effects observed in high-temperature superconductor compounds (HTSC's) in order to distinguish their dimensional and intrinsic properties. Before the discovery of HTSC's, the major part of works on the properties of layered superconductors was related to the study of the so-called dimensional crossover, occurring when the perpendicular coherence length $\xi_\perp(T)$ becomes comparable to the period of the layering.[1] More recently, the complicated nature of the $H$-$T$ phase diagram ($H$ is the external magnetic field and $T$ is the temperature) in the naturally layered HTSC's,[2] has given new impulse to the investigation of the vortex dynamics in multilayered superconductors, where it is possible to artificially control and change many parameters of the system.[3] One of the most interesting effects in the vortex properties of superconducting multilayers is the presence of peaks in the magnetic-field dependence of the superconducting critical current density $J_c$, first observed by Raffy *et al.* on Pb/PbBi proximity coupled multilayers.[4,5] This so-called peak effect has been also observed in conventional low-temperature superconducting materials,[6] layered $2H$-$NbSe_2$ single crystals,[7] and recently in HTSC's.[8] After Raffy *et al.* the peak effect has been measured in several artificially layered superconducting systems, such as Nb/Ta,[9] Nb/NbZr,[10] and Nb/Cu.[11] The first interpretation of this effect was given by Ami and Maki[12] in terms of commensurability between the multilayer period (that is constant) and the vortex lattice (VL) spacing (that depends on magnetic field). The original idea was initially contributed by Pippard,[13] who explained the peak effect in superconductors by the mechanism of the adjustment of the VL with pinning centers. This approach was refined by the theory of the collective pinning,[14] in which, due to the softening of the VL shear modulus $c_{66}$ with the increasing magnetic fields, above a certain critical field the strain exceeds the elastic limit in some part of the system, occurring in VL plastic deformations. This gives a decrease of the VL correlated volume with a fast increase of $J_c$. Other explanations of the peak effect in superconductors are related to the increase of the elementary pinning force while some precipitates, with increasing magnetic field, undergo the transition to the normal state,[7,15] to the crossover from elastic to plastic VL creep,[16] or to the transition from two-dimensional collective pinning to a three-dimensionally disordered state.[17,18] Generally, each of these models is able to explain only a part of the available experimental data and some of them[15,16] are not developed for the case of multilayered superconducting systems.

In this article we present experimental results of the vortex pinning investigation in Nb/Pd sputtered multilayers. $J_c$ measurements on Nb/Pd multilayers by means of magnetic torquemeter have been presented by de Groot *et al.*[19] Here we systematically performed transport measurements of the upper critical magnetic field $H_{c2}$, critical current density $J_c$, and pinning force $F_p$ on patterned Nb/Pd samples for both the perpendicular and the parallel orientation of the externally applied magnetic field at different Pd thicknesses and temperatures. The peak effect has been observed for parallel external magnetic fields at large Pd thicknesses, $d_{\mathrm{Pd}} > 100$ Å. The results are discussed comparing them with the existing theoretical approaches. Our data are consistent with the presence of matching effect of the vortex kinks present in the system with the periodic layered structure.

 

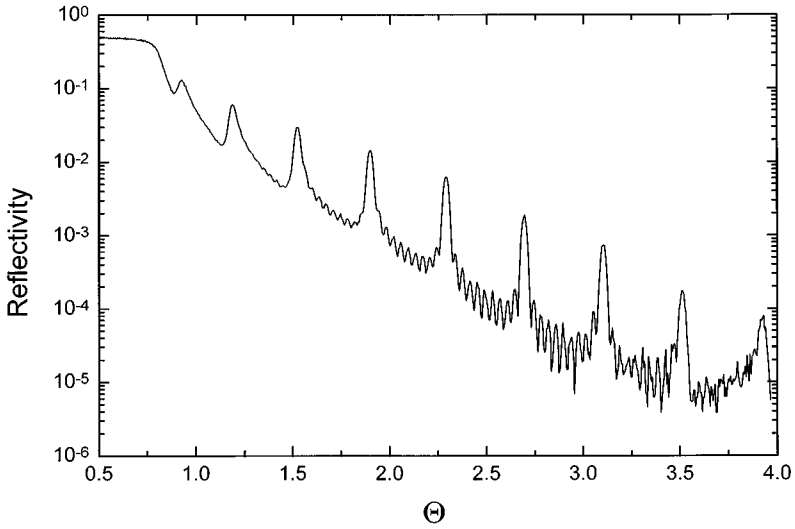


FIG. 1. Low angle x-ray-diffraction pattern for a typical Nb/Pd multilayer with Pd thickness of 20 Å. The Nb thickness is 187 Å.

## II. SAMPLE CHARACTERIZATION AND EXPERIMENTAL TECHNIQUES

Periodic Nb/Pd multilayers were deposited onto 3-in. Si(100) wafers using a magnetically enhanced dc triode sputtering gun for Pd and a magnetron gun for Nb.[20]

The Si wafers were let to pass alternatively over Pd and Nb guns. Changing the time during which the substrate is exposed to the sputtered materials, samples with different Nb and Pd amounts have been obtained. All the samples had constant Nb thickness ($d_{\mathrm{Nb}}=187$ Å), while Pd thickness ($d_{\mathrm{Pd}}$) was varied from 17 to 170 Å. The layering of the samples was confirmed by low angle x-ray-diffraction (LAXRD) analysis. LAXRD has been performed both to check the multilayer quality and to obtain the values of the Nb and Pd thicknesses. Figure 1 showes a LAXRD pattern for a typical sample with $d_{\mathrm{Pd}}=20$ Å. Clear Bragg peaks appear at the angles where constructive interference occurs; in addition the presence of multiple satellite peaks, located between two main Bragg peaks, indicates the good layering of our samples. Fitting the LAXRD patterns to a Fresnel-type optical model yields the values of the Nb thickness, the Pd thickness, and of the interfacial roughness (always in the range 5–10 Å). All the samples studied were made of 10 Pd/Nb bilayers with an additional Pd layer on the top to avoid both Nb oxidation and surface superconductivity. The layering of the samples was also confirmed by depth profiling using Auger electron spectroscopy. Rutherford backscattering spectroscopy (RBS) analysis was also employed to cross-check for layer thicknesses. The thicknesses obtained from LAXRD and RBS analyses agree within a few percent.

The $H_{c2}$ and $J_c$ measurements for both the perpendicular and the parallel orientation of the magnetic field with respect to the plane of the films were done on patterned samples with the length $l=100$ $\mu$m and the width $w=15$ $\mu$m. The strips were obtained by usual photolithographic technique followed by chemical etching. The average etching rate was about 250 Å/s. The $H_{c2}$ values were measured at the half of the resistive transition, the width of which was less than 0.1 K in zero field. The applied dc bias current density was $\sim 1.5 \times 10^6$ A/m$^2$. The $J_c$ values were obtained from $I$-$V$ curves using a 1 $\mu$V criterion. The experimental technique allows us to apply bias current in two directions, always perpendicular to the orientation of the external magnetic field. For each sample the $J_c(H)$ dependencies were measured at different temperatures. The temperature stabilization was better than $10^{-2}$ K. The flux-pinning force density $F_p$, was defined in the usual way, $F_p=\mu_0|\mathbf{J_c}\times\mathbf{H}|$.

On the patterned samples we also measured the critical temperature $T_c$. The $T_c$ values scale well according to the deGennes-Werthamer proximity effect model,[21] confirming that our multilayers behave like proximity coupled superconducting-normal metal-superconducting (SNS) systems.

We present the results of systematic measurements for four samples, having different Pd thicknesses. The characteristic sample parameters are summarized in Table I.

## III. PERPENDICULAR MAGNETIC-FIELD MEASUREMENTS

In this Section we present and discuss the measurements performed in the presence of external perpendicular magnetic field. The results indicate that the mechanism responsible for the vortex pinning is the same for all the samples and that this is related to a predominant contribution coming from grain boundaries.

TABLE I. Characteristic parameters of the measured samples. $d_{\mathrm{Nb}}$ is the thickness of Nb layer; $d_{\mathrm{Pd}}$ is the thickness of Pd layer; $\xi_{\parallel}(0)$ is the parallel coherence length at $T=0$; $\sqrt{M/m}$ is the anisotropic Ginzburg-Landau mass ratio at $T=0$; $\rho_{300\,\mathrm{K}}$ is the resistivity at $T=300$ K and $\rho_{10\,\mathrm{K}}$ is the resistivity at $T=10$ K.

| Sample | $d_{\mathrm{Nb}}$ (Å) | $d_{\mathrm{Pd}}$ (Å) | $T_c$ (K) | $\xi_{\parallel}(0)$ (Å) | $\sqrt{M/m}$ | $\beta=\frac{\rho_{300\,\mathrm{K}}}{\rho_{10\,\mathrm{K}}}$ |
|---|---|---|---|---|---|---|
| NP170 | 187 | 170 | 3.65 | 149 | 3.3 | 1.28 |
| NP132 | 187 | 132 | 4.00 | 141 | 2.3 | 1.25 |
| NP066 | 187 | 66 | 4.80 | 130 | 2.0 | 1.24 |
| NP017 | 187 | 17 | 7.00 | 93 | 1.4 | 1.55 |

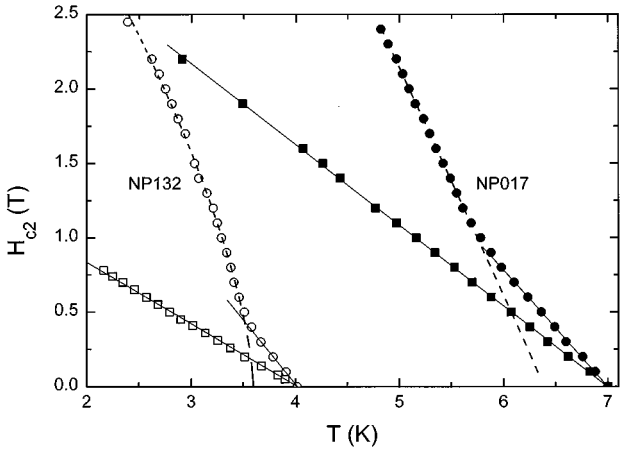


FIG. 2. The $H_{c2}$ vs temperature dependence for NP017 (close symbols) and NP132 (open simbols) multilayers. Squares correspond to the perpendicular magnetic field and circles to the parallel magnetic field. The solid lines represent the linear best fits to the experimental data. The dashed line represents the fit following from the relation $H_{c2}(T) \propto (1-T/T_c)^{\alpha}$.

In Fig. 2 the $H_{c2}(T)$ dependencies for sample $NP017$ (close symbols) with $d_{\mathrm{Pd}}=17$ Å and sample $NP132$ (open symbols) with $d_{\mathrm{Pd}}=132$ Å are shown. The squares correspond to the perpendicular field orientation. In all the measured range of temperatures and fields the upper perpendicular magnetic field $H_{c2\perp}(T)$ curves are linear. From the slope of these curves we have calculated the values of the zero temperature parallel superconducting coherence length $\xi_{\parallel}(0)$ reported in Table I, using the well-known Ginzburg-Landau expression

$$\xi_{\parallel}(0)=\sqrt{-\frac{\Phi_0}{2\pi T_c \left.\frac{dH_{c2\perp}}{dT}\right|_{T=T_c}}},$$

where $\Phi_0$ is the flux quantum and $T_c$ is the critical temperature of the sample.

The $J_c$ vs $H$ curves measured for all the samples in Table I at different temperatures were monotonically decreasing. In Fig. 3 we show the flux-pinning force density $F_p$ vs the perpendicular magnetic field measured on sample $NP170$ with $d_{\mathrm{Pd}}=170$ Å at five temperatures in the range $0.55<t=T/T_c<0.85$. Inset to Fig. 3 shows the normalized flux-pinning force $f=F_p/F_{p\max}$ ($F_{p\max}$ being the maximum value of the flux-pinning force density) vs the perpendicular reduced magnetic field $h=H/H_{c2}$. The $H_{c2}$ values have been defined as the field where the critical current density decreases to $5\times10^6$ $A/m^2$ and were in agreement within a few percent with the $H_{c2}$ values extracted from the resistive transition curves $R(T,H)$. The temperature scaling of the $f(h)$ dependencies indicates that the same pinning mechanism is present at all the investigated temperatures. The solid line in the inset to Fig. 3 is the best fit to the experimental data, and corresponds to the dependence $h^{0.9}(1-h)^{1.1}$, very close to the dependence $h(1-h)$ expected in the case of individually pinned vortices.[22,23] The linear field dependence of the normalized pinning force in the limit $h\to1$ is an indication that even close to $H_{c2\perp}$ the vortices do not form a lattice as it should be if the grain boundaries play a dominant role in the pinning. For low $T_c$ superconductors grain-boundary pinning becomes important at resistivity values $\rho$ higher than 10 $\mu\Omega$ cm.[9] In our samples, the $\rho$ values are in the range 15 $\mu\Omega$ cm–25 $\mu\Omega$ cm at $T=10$ K. From the value of $\mu_0 H_{c2\perp} \simeq 0.7T$ for sample $NP170$ at the lowest reached temperature (2.07 K) we get an average vortex spacing $a_0 \sim (\Phi_0/H)^{1/2} \sim 540$ Å that is of the same order of magnitude of the average dimensions of the grains as calculated by the Scherrer-Debye formula[24] from the x-ray-diffraction pattern. In Fig. 4 we show the normalized pinning force vs the reduced perpendicular magnetic field for all the samples investigated at the reduced temperature $t\simeq0.57$. The scaling of the curves, independently from the layering, reveals the same pinning

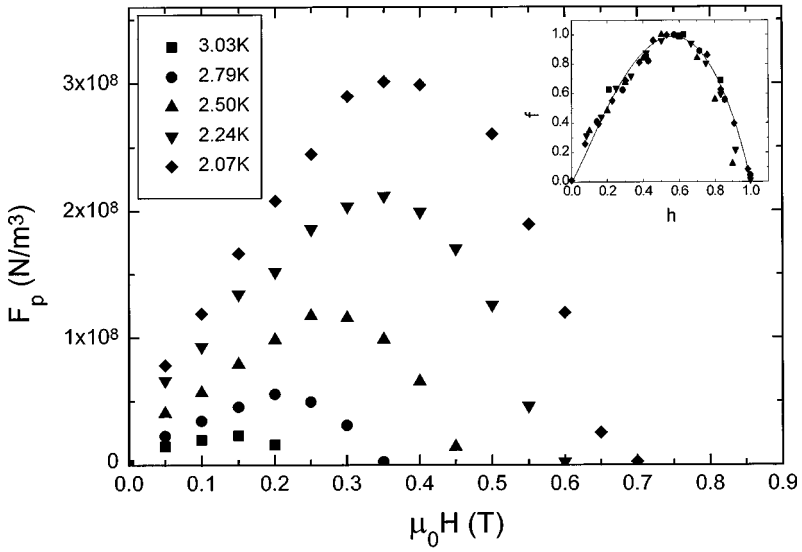


FIG. 3. The flux pinning force density $F_p$ vs perpendicular magnetic field $H$ for NP170 multilayer at five temperatures. Inset shows the normalized flux-pinning force $f=F_p/F_{p\,\max}$ vs the perpendicular reduced magnetic field $h=H/H_{c2}$. Symbols of the inset are the same as in the figure. The solid line is the fit to the data obtained from the relation $f(h)\propto h^{0.9}(1-h)^{1.1}$.

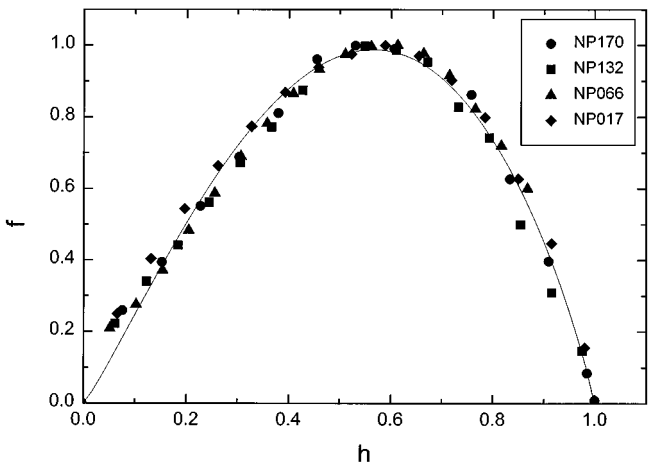


FIG. 4. The scaling of the normalized perpendicular flux-pinning force for four samples at $t=T/T_c\simeq 0.57$. The solid line is the fit to the data obtained from the relation $f(h)\propto h^{0.9}(1-h)^{1.1}$.

mechanism in all Nb/Pd multilayers in perpendicular magnetic field, confirming that the grain boundaries are the most effective pinning centers.

## IV. PARALLEL MAGNETIC-FIELD MEASUREMENTS

### A. Experimental results and discussion

We now focus on the measurements with external parallel magnetic fields. We first show the experimental data and compare them with the existing theories and then we develop a simple model that can explain the main features of the obtained data. In Fig. 2 the circles show the upper parallel critical magnetic field behavior $H_{c2\|}(T)$ for sample $NP132$ (open symbols) and for sample $NP017$ (close symbols). Both the curves present the well-known three-dimensional (3D)–two dimensional (2D) crossover, changing their dependence from linear to square root like below a certain temperature $T_{cr}$. This effect is related to the temperature dependence of the perpendicular superconducting coherence length $\xi_\perp(T)$. At $T\sim T_{\rm cr}$, $\xi_\perp(T_{\rm cr})$ is comparable to the period of the multilayer, determining the decoupling of the system and the appearance of the 2D behavior. At $T<T_{\rm cr}$ the expected dependence of $H_{c2\|}(T)$ should be square-root-like with $H_{c2\|}(T)\sim(1-T/T_c)^{1/2}$. The dashed lines in Fig. 2 are the best fits obtained from the expression $H_{c2\|}(T)\sim(1-T/T_c)^{\alpha}$. We have $\alpha\simeq 0.67$ for sample NP132 and $\alpha\simeq 0.98$ for sample NP017. This last value, very close to 1, is probably due to the relatively narrow temperature range at $T<T_{\rm cr}$, where the sample is not yet behaving completely 2D. On the other hand, the change in the temperature dependence of the $H_{c2\|}(T)$ curve is clear, indicating that, even in the case of the sample with $d_{\rm Pd}=17$ Å, we have reached the zone where the system starts to behave 2D.

It is known that for Josephson-coupled layered superconductors the 3D→2D crossover occurs when $\xi_\perp(T_{\rm cr})/\Lambda\sim 0.7$,[25] where $\Lambda=d_{\rm Pd}+d_{\rm Nb}$ is the multilayer period. In our SNS samples this ratio is always less ($\simeq 0.5$) than that predicted by the theory. Similar values ($\simeq 0.5$) were obtained for Nb/Ta (Ref. 26) and ($\simeq 0.4$) for V/Ag (Ref. 27) multilayers, indicating that for this type of systems the dimensional 3D→2D crossover occurs at lower temperatures than those expected for Josephson-coupled superconductors.

In Fig. 5 the $J_c$ vs $H$ curves for sample NP132 at different temperatures are shown. Below 3 K the $J_c(H)$ curves present a clear peak while at $T>3$ K the $J_c(H)$ curves are monotonic with a plateau developing for decreasing temperatures. A similar behavior has been observed for sample NP170 with $d_{\rm Pd}=170$ Å. It is interesting to point out that, for both the samples NP132 and NP170, the peak in the $J_c(H)$ curves is present at temperatures well below $T_{\rm cr}$, where the $H_{c2\|}(T)$ dependence is strongly nonlinear. On the other hand, for sample NP017 with $d_{\rm Pd}=17$ Å and for sample NP066 with $d_{\rm Pd}=66$ Å, as shown in Fig. 6, the $J_c(H)$ curves do not present a peak even at the lowest reached temperature, well below $T_{\rm cr}$. The field position of the peak in $J_c$ is temperature dependent. In Fig. 7 we have plotted the fields at which the peak is observed, $H_p$, vs the temperature $T$ for both the samples NP132 and NP170. The solid lines are the best fits

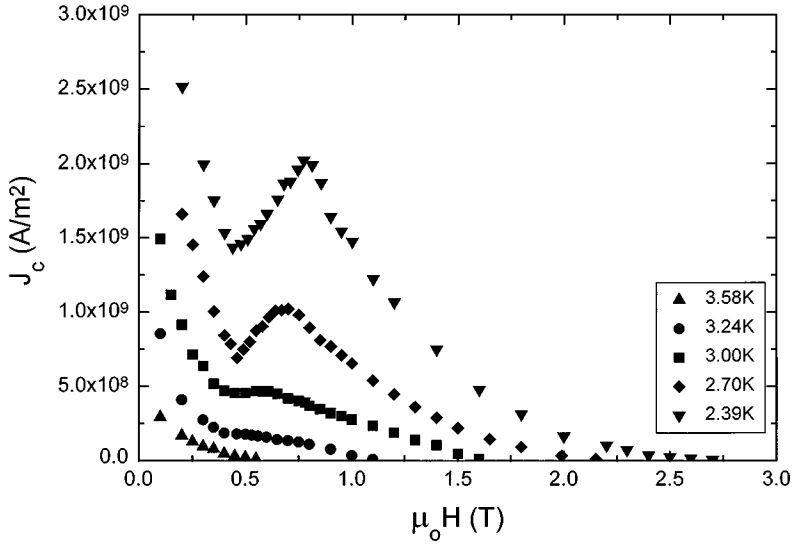


FIG. 5. The critical current density $J_c$ vs parallel field for NP132 sample at five temperatures.

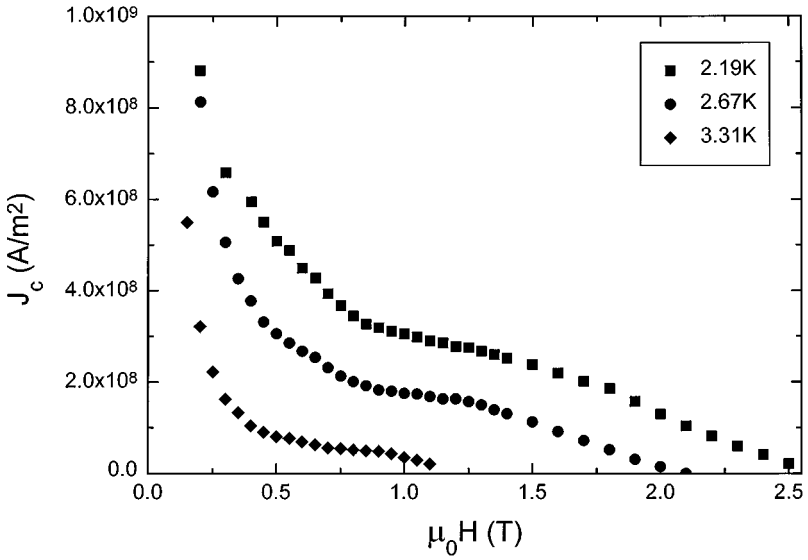


FIG. 6. The critical current density $J_c$ vs parallel field for NP066 sample at different temperatures.

calculated assuming $H_p(T) \sim (1-T/T_c)^{\beta}$. In both the cases $\beta \simeq 0.6$, very close to the value of the exponent $\alpha$ obtained for the temperature dependence of $H_{c2\|}(T)$ below $T_{\rm cr}$. Similar results have been observed in HTSC's,[28] where the peak position showed the same temperature dependence of the irreversibility field.

In Fig. 8 we show the normalized pinning force $f$ vs the reduced parallel magnetic field $h$ at different temperatures for sample NP170. The $f(h)$ curves for sample NP132 are similar to those presented in Fig. 8. All the curves of Fig. 8 scale well in the region of large $h$ values, while at small $h$ values the scaling is accomplished only for the curves taken at temperatures below 3 K. Below 3 K the $f(h)$ curves are typical of a strongly interacting vortex system at low fields ($h<0.5$) while at high fields ($h>0.5$) the $f(h)$ behavior is that related to noninteracting (individually) pinned vortices.[22,23] Above 3 K the curves present a plateau when $h \to 0$.

We now compare the experimental data with the existing theoretical models. The large part of these models is based on the matching of the vortex lattice with other periodic structures present in the system, but, especially after the discovery of the HTSC's, new mechanisms have been proposed to explain the presence of a peak in the $J_c(H)$ curves. For example, as it was recently shown,[16] a possible origin of the peak effect observed in HTSC's could be the crossover from elastic creep of vortices at low magnetic field to plastic creep at high magnetic field. According to this explanation, $H_p$ should be temperature dependent with a dependence determined by that of the vortex line tension $\epsilon_0$, namely, $H_p(T) \sim \epsilon_0(T) \sim \lambda(T)^{-4} \sim [1-(T/T_c)^4]^2$. Therefore, this model gives the $H_p(T)$ dependence with an upward curvature, while in our case the measured $H_p(T)$ curvature is downward.

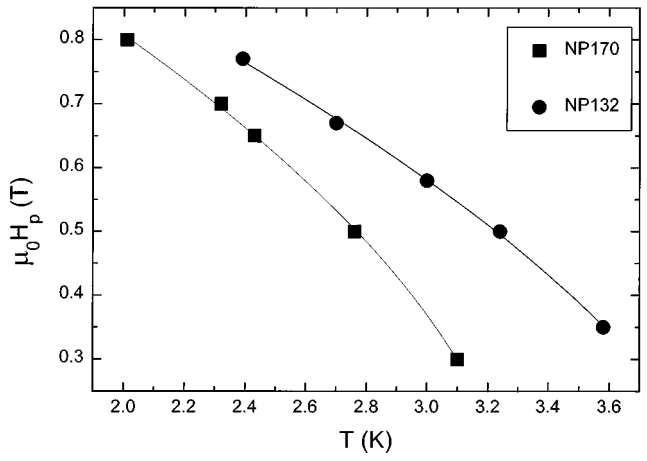


FIG. 7. The dependence of the peak field $H_p$ vs the temperature $T$ for two samples. The solid lines are the fits to the data obtained from the relation $H_p(T) \propto (1-T/T_c)^{\beta}$ with $\beta \simeq 0.6$.

Another model developed by Kugel *et al.*[15] in the case of a superconductor with normal inclusions, is able to explain the peak effect in superconducting multilayers, even though it is intended to be applied directly in the case of bulk HTSC's. In their approach Kugel *et al.* relate the presence of the peak effect to a sudden increase of the elementary pinning force due to the suppression of superconductivity by the external magnetic field in the normal inclusion (Pd layers). At low magnetic fields, the extension, due to the proximity effect, of the superconducting wave functions in the normal zones (Pd layers) is large, so that the order parameter is only weakly suppressed and the difference $\Delta F$ between the free energy in the normal zones (Pd layers) and in the superconducting zones (Nb layers) is small. At high fields, the order parameter decays faster in the normal zones than in the superconducting parts, so that $\Delta F$ increases. The pinning force is obviously proportional to $\Delta F$, therefore increasing with increasing fields. This model gives a temperature dependence of $H_p$ related to that of the superconducting parameters in the normal zones and qualitatively describes the observed temperature behavior of the pinning forces. On the other hand, according to Kugel *et al.*, the peak effect should be present only in systems where $d_n > \xi_s$ ($d_n$ is the dimension of the normal inclusions and $\xi_s$ is the coherence length in the superconducting zones) while in our Nb/Pd multilay-

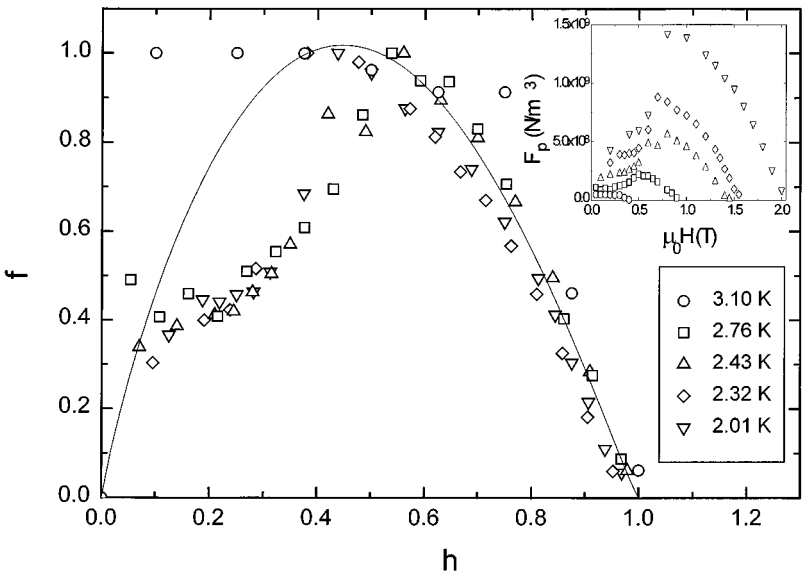


FIG. 8. The normalized flux-pinning force $f=F_p/F_{p\,\max}$ vs perpendicular reduced magnetic field $h=H/H_{c2}$ for the sample NP170 for five temperatures. The solid line is the fit to the data obtained from the relation $f(h)\propto h^{1.1}(1-h)^{1.0}$. In the inset: the flux-pinning force density $F_p$ vs the parallel magnetic field at different temperatures for the same sample. The symbols are the same as in the figure.

ers we have observed it even in the case of $d_n=d_{\mathrm{Pd}}\sim\xi_s(T)/2$. Finally, the intrinsic pinning assumed in the model, should give high critical current densities in the region of peak effect,[2] at least two orders of magnitude larger than those measured in our samples, where $J_c\sim10^5$ A/cm$^2$.

In trying to explain our experimental data, we have, therefore, turned our attention to the theories based on matching effects. One of the first proposed is that of Ami and Maki,[12] based on the matching between the vortex system and the multilayer periodicity. According to Ami and Maki, the matching fields for the peak effect are given by

$$\mu_0 H_{m,n}=\frac{\sqrt{3}\Phi_0}{2\Lambda^2}\,\frac{1}{n^2+m^2+nm}, \tag{1}$$

where $n,m=1,2,3\ldots$ . The possible values of the matching fields for the sample NP132 do not correspond to the observed values in Fig. 5.

Another model, in which the peak position is related to a matchinglike mechanism, is that proposed by Brongersma *et al.*[11] According to this model, the formation of vortex structure in multilayered superconductors in parallel magnetic field is not governed by the periodic layering but by the rearrangements of the parallel vortex system, during which an increasing number of vortex chains is formed. In this case the peaks should occur at fields

$$\mu_0 H_N=\frac{\sqrt{3}}{2}\,\Phi_0\,\frac{\xi_\perp}{\xi_\parallel}\left(\frac{N}{D}\right)^2, \tag{2}$$

where $D$ is the total thickness of the sample and $N=2,3,4,\ldots$ is related to the number of vortex chains. This model has been developed to explain the peak effect observed in Nb/Cu multilayers with very low values of the anisotropic Ginzburg-Landau mass ratio, $M/m\simeq1.4$. In our case, for the samples in which we observed the peak effect, the values of $M/m$ were higher than 4 and there was not agreement between the field values calculated from Eq. (2) and those observed.

Koorevaar *et al.*[10] measured a $H_p(T)$ dependence similar to that of the $H_{c2\parallel}(T)$ on Nb/NbZr multilayers. The presence of the peak effect in their system was tentatively explained assuming VL phase reconstruction when the dimensionality of the system goes from 3D to 2D. According to Ref. 10, the peak in $J_c$ should be due to a change in the topology of the vortices in the system from rigid bars to perpendicular pancakes connected by parallel strips. This model assumes that, even in the case of parallel field measurements, there is always a finite perpendicular component of the external field due to small misalignment that determines the presence of perpendicular pancake vortices. This interpretation qualitatively explains the $H_p(T)$ dependence and the $f(h)$ curves scaling below a certain temperature. In fact, the $H_p(T)$ dependence is directly related to the 3D→2D crossover of the $H_{c2\parallel}(T)$ curves, while the $f(h)$ curves should be related to strongly interacting vortices at fields below $H_p$, while at high fields ($h\rightarrow1$) the pancakes should be less interacting with each other. The approach given in Ref. 10 does not explain why the peak effect in our Nb/Pd multilayers is observed only when $d_{\mathrm{Pd}}>100$ Å, even though in the case of the samples NP066 and NP017, respectively, with $d_{\mathrm{Pd}}=66$ Å and 17 Å a 3D→2D crossover in the $H_{c2\parallel}(T)$ curves is observed.

Joining the idea of the presence of vortex kinks in our layered system with that of matching effects with the artificial periodic structure, we have developed a model that describes the field position of the peaks and the observed $J_c(H)$ dependence close to the peaks also taking into account the observed temperature scaling of the pinning forces. A qualitative explanation of the temperature dependence of the $H_p$ values is also proposed.

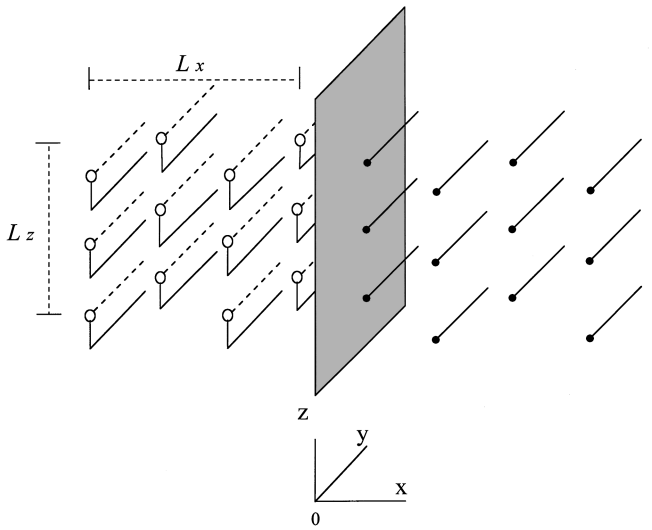


FIG. 9. Sketch of the vortex structure in the multilayers in parallel field. $L_x$ and $L_z$ are the lengths within which kinked vortices appear.

### B. The model

In a Nb/Pd multilayer, the resistance due to the motion of vortices across the layers should result in high critical current densities ($J_c \sim 10^7 - 10^8$ A/cm$^2$) because of strong intrinsic pinning.[2] On the other hand, the motion of vortex kinks in the magnetic field direction will give a resistive state with lower $J_c$ values ($\sim 10^4 - 10^5$ A/cm$^2$). For the orientation of the magnetic field parallel to the layers, kinks can enter the sample through imperfectness at the sample edges.

Suppose layers to be in the $x$-$y$ plane and the magnetic field $H$ is directed along the $y$ axis while the current $I$ is along the $x$ axis. The imperfectness at the sample edges determines sizes $L_x$ and $L_z$ of the kink region in Fig. 9. The energy of the system consists of the Lorentz energy

$$E_L = -\frac{\phi_0 \Lambda}{c} J\left(\frac{L_x L_z}{\phi_0} H\right) y, \tag{3}$$

where $J$ is the current density and $\Lambda$ is the structure period along the $z$ axis, and of the elastic energy $E_{\rm el}$ that originates from the mismatch of vortex lattices at $x<0$ and $x>0$. The dashed lines at $x<0$ represent the unshifted vortex lattice which matches the $x>0$ system.

The matching magnetic field is determined by the condition

$$H_p = \frac{\sqrt{3}}{2} \frac{\phi_0}{\lambda_J \Lambda}, \tag{4}$$

where $\lambda_J = \Lambda\, \lambda_z/\lambda_{xy}$ is the Josephson length and $\lambda_z/\lambda_{xy} = \sqrt{M/m}$. At $H>H_p$ vortices fill in the layers with a high population and the elastic energy density $\epsilon$ acquires the additional small factor $(H_p/H)^2$ so that $\epsilon \sim (\phi_0 H_p)/(\lambda_{xy}\lambda_z)(H_p/H)^2$.[29] The scale $x_0$ along the $x$ axis becomes $x_0 = \lambda_J H_p/H$. The elastic energy can be estimated now as

$$E_{\rm el} \approx \epsilon x_0 L_z y \approx \left(\frac{\phi_0}{4\pi\lambda_{xy}}\right)^2 \frac{H_p}{H} \frac{L_z}{\Lambda} y. \tag{5}$$

The critical current density can be obtained from the condition of force equilibrium

$$\frac{\partial}{\partial y}(E_L + E_{\rm el}) = 0, \tag{6}$$

which reads, by means of Eqs. (3) and (6), and for $H_p<H$

$$J_c = J_{c0}\left(\frac{H_p}{H}\right)^2, \tag{7}$$

with

$$J_{c0} \approx \frac{c\phi_0}{(4\pi\lambda_{xy})^2 L_x}. \tag{8}$$

At $H<H_p$ the matching condition is violated and the vortex system can adjust itself to the layered structure, for example by creation of point dislocations with the concentration $(H_p - H)/H_p$. This increases the energy density of the vortex system (compared with the equilibrium Abrikosov lattice) by the amount $\phi_0 H/\lambda_{xy}\lambda_z\, H_p - H/H_p$. Another possibility to organize vortex system below $H_p$ is to slide vortices along the layers forming a rare lattice. In contrast to the previous possibility the energy density pay is less, namely, $\approx(\phi_0 H/\lambda_{xy}\lambda_z)[(H_p - H)/(H_p)]^2$.[30] This makes the second possibility more preferable at least at not high $H_p - H/H_p$ values. For such a stretched lattice the energy of the boundary at $x=0$ in Fig. 9 is proportional to $e^{iq_x a}$ where $a = \phi_0/H\Lambda$ is the period along the $x$ axis, the wave vector $q_x = i\,\lambda_{xy} q_z/c$ and, for a triangular lattice, $q_z = \pi/\alpha$. This allows to estimate the boundary energy as

$$E_{\rm el} \propto \frac{\phi_0^2 L_z}{\lambda_{xy}\lambda_z \Lambda}\, e^{-\pi a/\lambda_J} y. \tag{9}$$

Differentiating the sum of Eqs. (3) and (9) with respect to $y$ one gets the critical current density for $H<H_p$

$$J_c \approx J_{c0}\, \frac{H_p}{H} \exp\left[\frac{2\pi}{\sqrt{3}}\left(1 - \frac{H_p}{H}\right)\right]. \tag{10}$$

Expressions (8) and (10) give the shape of the matching peak shown in Fig. 10 which very well describes the observed experimental behavior (Fig. 5), while Eq. (4), using the data in Table I, gives exactly the observed value of $H_p$ (0.77 T) in the case of the Nb/Pd sample with $d_{\rm Pd} = 132$ Å. Moreover, the change of the vortex structure across $H_p$ also accounts for the unusual behavior of the pinning forces at high ($h \to 1$) and low ($h \to 0$) magnetic fields, using an argument similar to that proposed by Koorevar *et al.*[10] Finally, this model also explain the absence of peak effect when $d_{\rm Pd} < 100$ Å. In these samples, in fact, Eq. (4) gives $H_p$ values higher than or comparable to $H_{c2}$. Moreover, at lower $d_{\rm Pd}$ values the typical dimension of the Abrikosov vortices ($\sim \sqrt{\xi_\perp \xi_\parallel}$) starts to be comparable to or higher than the Pd layer thickness, rendering uneffective their pinning strength. The position of the matching field $H_p$ is temperature independent in the ideal case but in reality perfectness of the vortex lattice is violated and the matching peak in $J_c(H)$ is smeared out the more the closer the temperature to $T_c$. The experimentally observed $J_c$ is contributed by the two mecha-

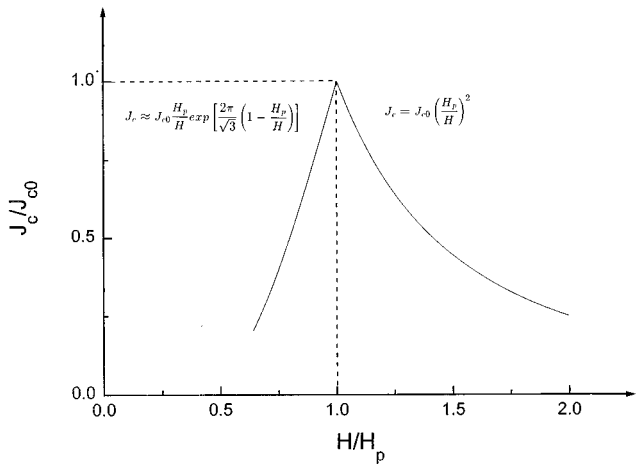


FIG. 10. Normalized critical current density as a function of normalized magnetic field calculated according to Eqs. (7) and (10).

nisms: matching effect $[J_c^{(m)}]$ and a pinning of moved vortex kinks in superconducting (Nb) part of layers $[J_c^{(\mathrm{pin})}]$, so

$$J_c = J_c^{(m)} + J_c^{(\mathrm{pin})}, \tag{11}$$

where $J_c^{(\mathrm{pin})}(H)$ decreases with the increase of $H$. This results in a shift of the observed peak position toward lower magnetic field under increase of temperature.

## V. CONCLUSIONS

We performed a systematic study of the vortex dynamics in Nb/Pd multilayers. The data obtained in the case of external perpendicular magnetic field indicate the presence of strong pinning centers located at the grain boundaries. In the parallel magnetic field at $t<0.9$ the peak effect in $J_c(H)$ dependencies has been observed in samples with large ($d_{\mathrm{Pd}}>100$ Å) Pd layer thicknesses. Our comparison of the experimental data with the available theories indicates that the origin of the critical current increase at some magnetic fields should be related to the matching of vortex kinks with the periodic structure of the system. We have developed a model based on this matching which takes into account the main observed features and describes accurately the $J_c(H)$ dependence close to $H_p$.

## ACKNOWLEDGMENTS

J.M.S. and C.M.F. were supported by ONR grant under Contract No. N00001492J1159. S.L.P. was partially supported by the Belarus Basic Research Foundation.

[1] B. Y. Jin and J. B. Ketterson, Adv. Phys. **38**, 189 (1989).
[2] G. Blatter, M. V. Feigelman, V. B. Geshkenbein, A. I. Larkin, and V. M. Vinokur, Rev. Mod. Phys. **66**, 1125 (1994).
[3] A. N. Lykov, Adv. Phys. **42**, 263 (1993).
[4] H. Raffy, J. C. Renard, and E. Guyon, Solid State Commun. **11**, 1679 (1972).
[5] H. Raffy, J. C. Renard, and E. Guyon, Solid State Commun. **14**, 427 (1974).
[6] A. M. Campbell and J. E. Evetts, Adv. Phys. **21**, 327 (1972).
[7] P. Koorevaar, J. Aarts, P. Berghuis, and P. H. Kes, Phys. Rev. B **42**, 1004 (1990).
[8] M. Daeumling, J. M. Seuntjens, and D. C. Larbalestier, Nature (London) **346**, 332 (1990).
[9] P. R. Broussard and T. H. Geballe, Phys. Rev. B **37**, 68 (1988).
[10] P. Koorevaar, W. Maj, P. H. Kes, and J. Aarts, Phys. Rev. B **47**, 934 (1993).
[11] S. H. Brongersma, E. Verweij, N. J. Koeman, D. G. de Groot, R. Griessen, and B. I. Ivlev, Phys. Rev. Lett. **71**, 2319 (1993); Thin Solid Films **228**, 201 (1993).
[12] S. Ami and K. Maki, Prog. Theor. Phys. **53**, 1 (1975).
[13] A. B. Pippard, Philos. Mag. **19**, 217 (1969).
[14] A. I. Larkin and Yu. N. Ovchinnikov, J. Low Temp. Phys. **34**, 409 (1979).
[15] K. I. Kugel, T. Matsushita, E. Z. Melikhov, and A. L. Rakhmanov, Physica C **228**, 373 (1994).
[16] Y. Abulafia, A. Shaulov, Y. Wolfus, R. Prozorov, L. Burlachkov, Y. Yeshurun, D. Majer, E. Zeldov, H. Wuhl, V. B. Geshkenbein, and V. M. Vinokur, Phys. Rev. Lett. **77**, 1596 (1996).
[17] E. H. Brandt, J. Low Temp. Phys. **64**, 375 (1986).
[18] R. Wördenweber and P. H. Kes, Phys. Rev. B **34**, 494 (1986).
[19] D. G. de Groot, A. J. Vermeer, C. W. Hagen, T. A. M. Schröder, N. J. Koeman, J. H. Rector, and R. Griessen, Vacuum **41**, 1244 (1990).
[20] L. Maritato, C. M. Falco, J. Aboaf, and D. I. Paul, J. Appl. Phys. **61**, 1588 (1987).
[21] P. G. deGennes and E. Guyon, Phys. Lett. **3**, 168 (1963); J. J. Hauser, H. C. Theuerer, and N. R. Werthamer, Phys. Rev. **136**, A637 (1964).
[22] E. H. Brandt, Phys. Lett. **77A**, 484 (1980).
[23] E. J. Kramer, J. Appl. Phys. **44**, 1360 (1973).
[24] H. P. Klug and L. E. Alexander, *X-Ray Diffraction Procedures*, 2nd ed. (Wiley, New York, 1974), Ch. 9.
[25] R. A. Klemm, M. R. Beasley, and A. Luther, J. Low Temp. Phys. **16**, 607 (1974).
[26] P. R. Broussard and T. H. Geballe, Phys. Rev. B **37**, 60 (1988).
[27] K. Kanoda, H. Mazuki, T. Yamada, N. Hosoito, and T. Shinjo, Phys. Rev. B **33**, 2052 (1986).
[28] A. A. Zhukov, H. Küpfer, G. Perkins, L. F. Cohen, A. D. Caplin, S. A. Klestov, H. Claus, V. I. Voronkova, T. Wolf, and H. Wühl, Phys. Rev. B **51**, 12 704 (1995).
[29] L. N. Bulaevskii, D. Dominguez, M. P. Maley, A. R. Bishop, and B. I. Ivlev, Phys. Rev. B **53**, 14 601 (1996).
[30] B. I. Ivlev, N. B. Kopnin, and V. L. Pokrovsky, J. Low Temp. Phys. **80**, 187 (1990).